ЖЭТФ, 2008, том 134, вып. 6 (12), стр. 1181–1194

PROCESSES INVOLVED IN THE FORMATION OF SILVER CLUSTERS ON SILICON SURFACE

S. R. Bhattacharyya [a], ***T. K. Chini*** [a], ***D. Datta*** [a],
R. Hippler [b], ***I. Shyjumon*** [b], ***B. M. Smirnov*** [c*]

[a] *Surface Physics Division, Saha Institute of Nuclear Physics 700064, Kolkata, India*

[b] *Institut für Physik, Ernst-Moritz-Arndt Universität Greifswald 17487, Greifswald, Germany*

[c] *Joint Institute for High Temperatures, Russian Academy of Sciences 125412, Moscow, Russia*

Received March 25, 2008

We analyze scanning electron microscopy measurements for structures formed in deposition of solid silver clusters onto a silicon(100) substrate and consider theoretical models of cluster evolution onto a surface as a result of diffusion and formation of aggregates of merged clusters. Scanning electron microscopy (SEM) attached with energy dispersive X-ray spectrometry (EDX) measurements of the formed films are presented. Solid silver clusters are produced by a DC magnetron sputtering source with a quadrupole filter for selection of cluster sizes (4.1 nm and 5.6 nm or 1900 and 5000 atoms per cluster in this experiment); the energy of cluster deposition is 0.7 eV/atom. Rapid thermal annealing of the grown films allows analyzing their behavior at high temperatures. The results exhibit formation of cluster aggregates via the process of diffusion of deposited solid clusters along the surface; an aggregate consists of up to hundred individual clusters. This process is essentially described by the DLA (diffusion-limited aggregation) model, and thus a grown porous film consists of cluster aggregates joined by bridges. Subsequent annealing of this film leads to its melting at temperatures lower than the melting point of bulk silver. The analysis of evaporation of this film at higher temperatures gives the binding energy in bulk silver $\varepsilon_0 = (2.74 \pm 0.03)$ eV/atom.

PACS: 36.40.-c, 36.40.Sx, 61.43.Hv, 68.35.B-, 68.37.Hk

1. INTRODUCTION

We aim to formulate the character of processes in the course of deposition of solid clusters onto a surface. Because there is a restricted number of models describing the character of these processes, the comparison of results of these models and experiments allows choosing appropriate models and their parameters to describe the behavior of solid clusters deposited on a surface, as well as the parameters of such models on the basis of certain measurements. We do this for deposition of solid silver clusters onto a silicon substrate, and our models relate to this case.

From the standpoint of the description of deposition processes, there is an analogy between solid cluster growth and the deposition of atoms on a surface [1, 2], if deposited atoms do not form chemical bonds with surface atoms. We assume that the individuality of solid clusters is preserved in the course of their deposition onto a surface and subsequent evolution. This means that only a small surface cluster layer takes part in the formation of chemical bonds between a solid cluster and a surface and also between clusters. We assume that the binding energy between clusters exceeds that between a solid cluster and a surface. Therefore, af-

*E-mail: bmsmirnov@gmail.com

ter deposition on a surface, a solid cluster may displace along the surface as a result of diffusion and form chemical bonds with other clusters, leading to a decrease in the cluster diffusion coefficient.

If the intensity of a cluster beam is small, evolution of clusters on a surface is described by the model of deposition diffusion aggregation (DDA) [3]; as a result of this process, fractal aggregates are formed on the surface consisting of solid clusters [4]. This model is based on the diffusion-limited aggregation (DLA) model [5–8], which assumes all the clusters to be collected in one aggregate. At high intensities of deposited clusters, the fractal structure of a deposited substance is lost, but the forming film has a porous structure, and its formation processes coincide with those for the above models. Hence, the elements of these models can be used in the analysis of formation and growth of a dense porous film resulting from deposition of solid clusters on a surface.

The analysis of the above processes is accompanied by experimental study of the deposition of silver cluster onto a silicon surface. This process is of interest for modern nanotechnology [9, 10]. Indeed, it is known since long ago that silver is an effective antibacterial remedy that kills microbes [11–13]. Special study [14] proves that the strongest action on bacteria corresponds to nonuniformities of silver surface of 1–10 nm. Just such a size of structural elements relates to a porous film that results from deposition of clusters on a surface if these clusters are formed in a gas discharge source. This means that in this case, silver is a catalyst of biochemical reaction for the distribution of size nonuniformities in the nanometer scale. Evidently, processes of the same character occur in applications when a metal surface is used as a catalyst in chemical production. Thus, in considering the physics of the cluster processes on a surface, we bear in mind that these processes are of interest for modern nanotechnology [15, 16]. In this context, optical and electric properties of silver and silver oxide clusters are used in contemporary micro- and nanoelectronics [17].

We note that these films resulting from deposition of solid magnetic clusters onto substrate may be of interest as a magnetic material. Indeed, the clusters in such films partly preserve their individuality, and can be regarded as individual domains in magnetic materials. Because the size distribution function of deposited clusters can be narrow, this allows obtaining magnetic materials with resonant parameters that depend on cluster sizes in a cluster beam. For natural magnetic materials with a wide size distribution function of domains, this is impossible.

2. CHARACTER OF THE INTERACTION OF SOLID CLUSTERS ON A SURFACE

In analyzing the evolution of solid clusters deposited on a surface, we are guided by the case of deposition of solid silver clusters onto a silicon surface and assume the same hierarchy of interactions in the cluster–surface system. We assume that solid clusters have an almost spherical shape and only a small part of surface atoms take part in the formation of a strong chemical bond between two clusters or clusters with the surface. Therefore, a major part of cluster atoms do not change their positions either in formation of cluster bonds or after the formation when the cluster is bound with other clusters or with the surface.

Next, clusters are compact systems of atoms, whereas cluster aggregates are porous systems because the major part of atoms preserve their positions in cluster aggregates. The compactness of individual solid clusters of silver has been investigated experimentally in [18, 19]. The mass of an individual cluster can be measured by two methods. First, we use a quadrupole mass spectrometer as a filter in generation of a mass-selected cluster beam, i.e., the cluster mass follows from the mass-spectrometric measurement. Second, when an individual atom is placed onto a surface, its size can be measured by microscopy. If we assume that the cluster density corresponds to a liquid drop, i.e., the cluster is compact, then we can find the cluster mass. Considering the compactness of our silver clusters deposited under similar conditions as in the experiment in [18], we can estimate the number of atoms in a cluster to be typically given by 10^3–10^5, which corresponds to usual sources of metal clusters.

We consider the regime of cluster deposition when the binding energy of two clusters is large compared to that between the cluster and surface. This determines the character of cluster evolution on the surface until this surface is more or less free. Attaching to a surface, a cluster is displaced over it as a result of diffusion. If two clusters encounter on a surface, they form a strong chemical bond, and hence this bond is preserved in the course of cluster evolution. Nevertheless, reconstruction of this bond is possible. This means that a common region of two clusters may change, i.e., two clusters may rotate with respect to others with the conservation of their common surface. In particular, an aggregate of clusters is formed in this way, and the number of nearest neighbors for an individual cluster in this aggregate is greater than two.

The clusters move over the surface under the action of thermal fluctuations. In this situation, a cer-

tain number of chemical bonds with the surface is preserved in the course of an individual movement, and as a result, the diffusion character of cluster motion is realized. We characterize this cluster motion by a typical distance a over which the direction of cluster motion changes and a typical time τ of traveling over this distance, and hence the cluster diffusion coefficient is $D \sim a^2/\tau$. We note that the typical distance a significantly exceeds the lattice constant of the surface for a large cluster.

Thus, the character of processes in the course of deposition of solid clusters onto a surface under the above conditions is as follows. Solid metal clusters of an almost spherical shape are deposited onto a surface and travel along it as a result of diffusion. Collision of clusters on the surface leads to formation and growth of cluster aggregates. In addition, the aggregates grow because solid clusters are deposited onto aggregates rather than a free surface. These processes lead to the formation of a porous film consisting of cluster aggregates. Our aim is to find the parameters of this process on the basis of experimental data for deposition of solid silver clusters onto a silicon surface and in this way to describe a general picture of the aggregate character of film growth as a result of deposition of solid metal clusters onto a neutral surface.

3. EXPERIMENTAL SETUP AND RESULTS

We briefly describe the main features of the experimental technique from the standpoint of the problem under consideration. There is a more detailed description of the used setup in previous papers [18–21]. For generation of a beam of silver clusters, a standard magnetron source of silver clusters [22] was used, with the clusters formed in the chamber of length 15 cm excited by a magnetron discharge of the power 100–200 W and cooled by liquid nitrogen. The vacuum system that includes a molecular turbo pump, backed and roughed by diaphragm pumps, can attain a vacuum of $\sim 8 \cdot 10^{-8}$ mbar in the deposition chamber.

A quadrupole mass filter (Quadrupole Mass Filter, QMF 200, Oxford Applied Research, Version 1.1) placed at the exit of the magnetron chamber selects clusters by masses. We assume solid clusters to be large and compact, and their density to coincide with that of a macroscopic solid. Assuming the cluster to be spherical, we express its radius as

$$r = r_W n^{1/3}, \tag{3.1}$$

where n is the number of cluster atoms and r_W is the Wigner–Seitz radius (for silver, $r_W = 0.166$ nm [23]). In this experiment, the diameters of selected silver clusters were $d = 2r = 4.1$ nm and $d = 5.6$ nm; according to formula (3.1), this corresponds respectively to $n = 1900$ and $n = 5000$ atoms per cluster. These clusters with the energy 0.7 eV/atom are deposited on a silicon target placed at the distance 32 cm from the exit of the magnetron chamber; the deposition time is 8 min. We note that the compactness of these silver clusters is confirmed by experiments in [18, 19], where the cluster mass and its size on a substrate were measured simultaneously.

Prior to the deposition of silver nanoclusters, substrates are prepared from the grown single crystalline Si wafers with (100) orientation polished on one side. In each experiment, these Si wafers were cleaned by etching with HF (Hydrofluoric) acid solution to remove the native oxide from the surface to ensure that bonding occurs between the silver atom of deposited cluster and the Si atom of the substrate wafer. However, after the cluster deposition, when such Si wafers were brought out of the deposition chamber, i.e., exposed to ambient conditions, native oxide is expected to form again on the substrates.

The deposited film of solid clusters is examined by a scanning electron microscope attached with energy dispersive X-ray analysis (SEM/EDAX) (model: Quanta 200 F). To obtain information about the height and lateral sizes of the deposited particles, an atomic force microscope (AFM) (model: NanoScope IV, Veeco Instr., USA) was used in the tapping mode under ambient condition using a Si tip having the resonance frequency 428 kHz. One of the silver clusters of deposited films was heat-treated by rapid thermal annealing (RTA) (model Jetfirst 100, Jipelec, Qualiflow, France). Figure 1*a* represents the SEM images of the morphology of a silver film with cluster sizes 5.6 nm for the deposition time 6 minutes at room temperature (300 K). The films were annealed in nitrogen atmosphere at the temperatures 473 K, 673 K, 873 K, and 1073 K for 3 minutes each; they are shown in Figs. 1*b* to 1*e*.

SEM measurement of the nanocluster films was accompanied by the analysis of energy dispersive X-ray spectrometry (EDX), which gives the elemental composition of a sample. This EDX technique essentially gives the electron spectrum resulting from ionization of internal electron shells of atoms by X-ray photons [24, 25] by detecting the characteristic X-rays of the elements present in a sample. We analyze the electron spectrum in a range of several hundred eV, depending on both the electron energy and the angle near a given resonance, with the typical exposition time 100 s. We note that the range of a fast electron in a medium is equal to [25]

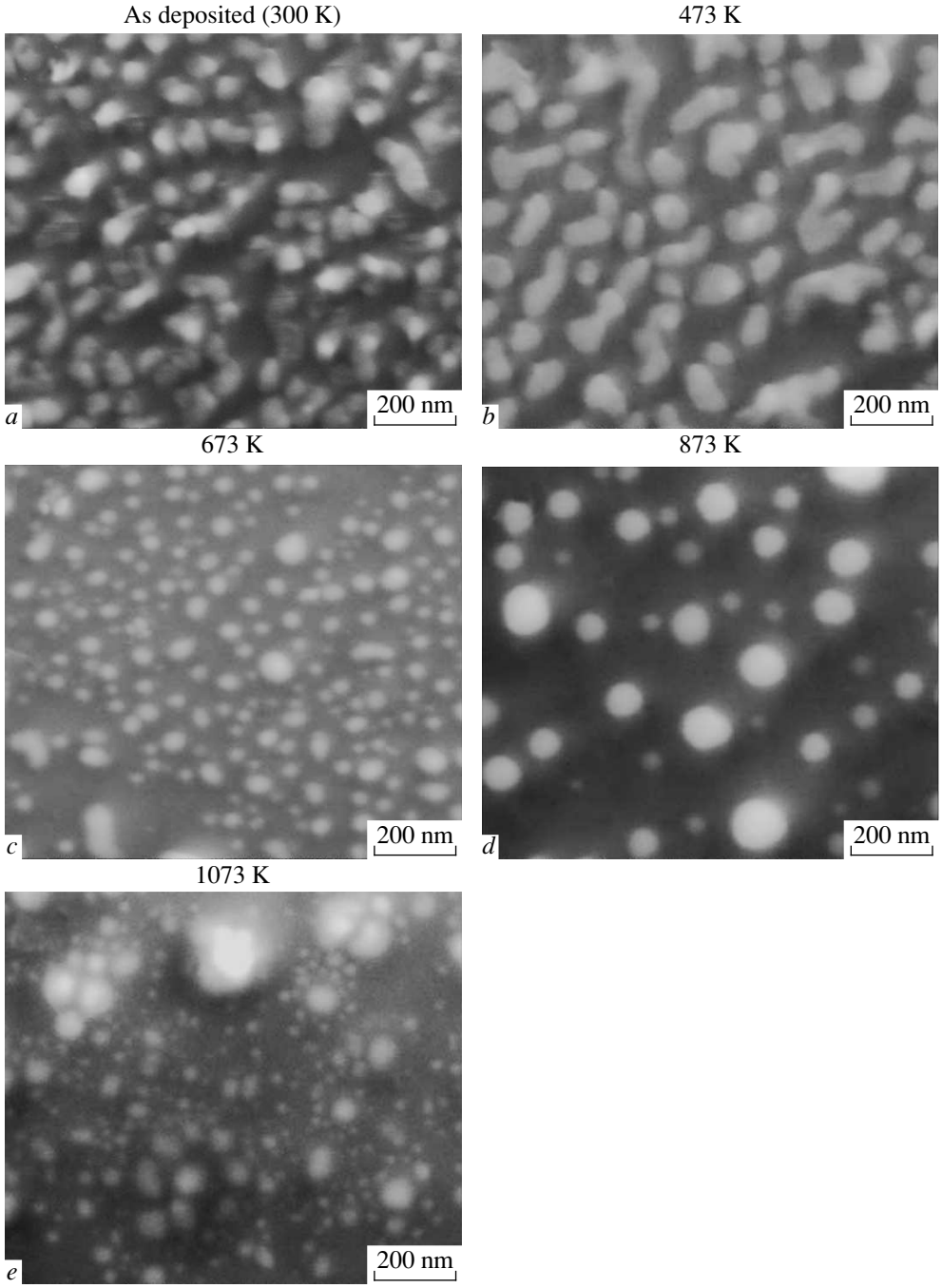

Fig. 1. Scanning electron microscopy (SEM) images of silver films formed on a silicon surface as a result of deposition of mass-selected silver clusters of 5.6 nm (a) at room temperature (300 K) and subsequently annealed at 473 K (b), 673 K (c), 873 K (d), and 1073 K (e) by rapid thermal annealing (RTA) set up for 3 minutes in nitrogen atmosphere in each case

$$\lambda(\text{nm}) = \frac{27.6A}{Z^{0.89}\rho} E_0^{1.67}, \qquad (3.2)$$

where A is the atomic weight, Z is the atomic number, ρ is the density given in g/cm^3, and E_0 is the average electron beam energy expressed in keV. Using X-ray photons from K-radiation of Al with the photon energy of the Al K_α line $\hbar\omega = 1486.6$ eV, the electron range in silver for electrons resulting from ionization of the Si atom is found to be $\lambda = 24$ nm at the energy 175 eV; for electrons from ionization of the K-shell of oxygen atoms of the energy approximately 50 eV, the range of Auger-ionization electrons is $\lambda = 3$ nm. As

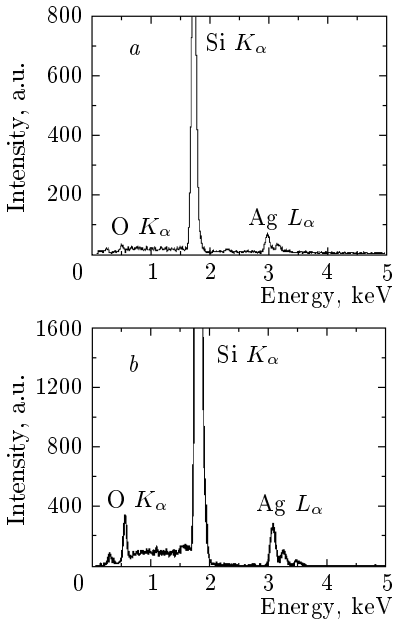

Fig. 2. Energy dispersive X-ray (EDX) spectrum of the film corresponding to SEM image in Fig. 1a (a) and SEM image in Fig. 1e (b)

is seen, a silver film screens electrons formed in Auger ionization of oxygen atoms bound with silicon atoms. These measurements exhibit the absence the oxidation of silver clusters in contrast to the titanium case [20]. As a result of annealing of the film at the temperature 1073 K, an intense signal of SiO_2 is observed both due to a more intensive silicon oxidation and because of an increase in the transparency of the silver film.

Figure 2 gives the EDX spectra of deposited silver films with the diameter 4.1 nm for incident solid silver clusters and different exposition times of clusters. The energy of X-ray photons is 5 keV in this experiment. The prominent peaks in the EDX spectra correspond to an L_α excitation in silver, K_α excitation in silicon, and K_α excitation in oxygen. Aggregates formed from larger solid clusters 5.6 nm in diameter are characterized by a larger silver content than those consisting of solid clusters 4.1 nm in diameter. These measurements definitely prove the absence of silver oxidation in the course of deposition, whereas oxidation proceeds in the case of deposition of Ti clusters [20].

As discussed above, solid clusters deposited on a silicon surface under conditions of this experiment propagate along the surface as a result of diffusion and merge in cluster aggregates as a result of cluster attachment to each other and the reconstruction of a forming aggregate with an increase in the number of contacts between neighboring clusters. SEM measurement allows estimating the geometrical size of the formed aggregates. As a result, we can find the size distribution function of aggregates. Subsequent formation of bridges between neighboring aggregates leads to formation of a continuous film. The regime of deposition in this experiment is such that the average film thickness does not exceed the diameter of a typical aggregate, and hence a major part of the film mass is concentrated in individual aggregates. Within some accuracy, we can therefore represent a deposited film as consisting of individual aggregates, and the parameters of individual aggregates and their size distribution function give the total film description.

Based on this model of film deposition, we give its parameters as a result of the complete experiment on morphology. For this, an AFM analysis of the samples was conducted. A representative diagram of AFM studies is shown in Fig. 3. The root-mean-square (RMS) roughness of the film was found to be 5.8 nm and the average height of the features was $\sim$ 27 nm. Comparing vertical diameters of aggregates from AFM measurements and their transverse (lateral) diameters on the basis of SEM measurements, we find that aggregates are flattened, and their transverse diameter exceeds the vertical diameter by up to 40 %. This means that the restructuring time of aggregates is comparable to a typical time of attachment of new clusters to an aggregate. Below, for simplicity, we assume aggregates to be spherical, which corresponds to a relatively small time of restructuring. In Figs. 4 and 5, we give the size distribution functions of aggregates resulting from joining of solid silver clusters of diameters 4.1 nm and 5.6 nm at identical exposure times. We note that the statistics of these aggregates do not allow determining the form of the distribution function, and we assume it to be Gaussian. Figure 6 contains the same size distribution function if a deposited film in Fig. 5 is heated up to 873 K and remains at this temperature for 3 min. Then aggregates soften and partially melt, such that after melting the bridges between them are transformed into almost round drops, and their size increases. All this is used below for the analysis of processes of formation and evolution of cluster aggregates resulting from deposition of solid silver clusters onto a silicon surface.

4. MODELS OF EVOLUTION OF DEPOSITED CLUSTERS ON A SURFACE

Below, we consider simple models describing cluster deposition on a surface. In this consideration, we assume the surface to be amorphous and clusters not to change bonds between surface atoms. But clusters form chemical bonds at the points of their contact with

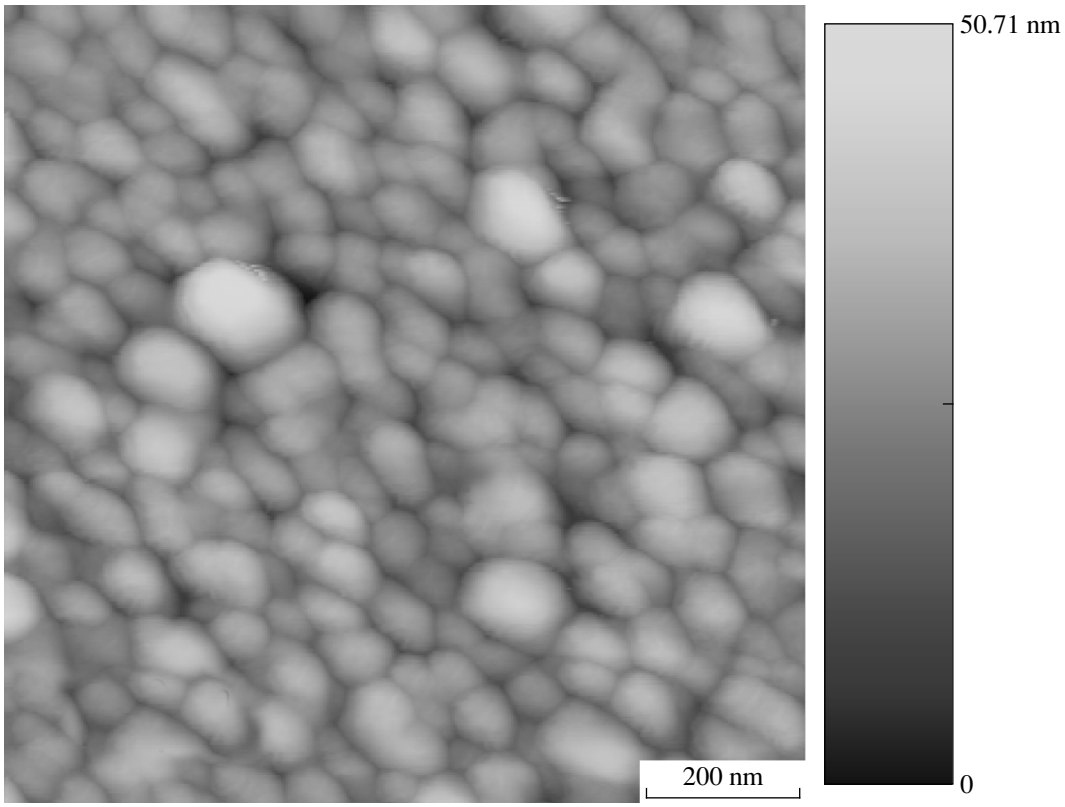

Fig. 3. Atomic force microscopy image of a silver film formed on the Si substrate by 5.6 nm clusters for the deposition time 6 minutes corresponding to the sample presented in Fig. 1*a*. The scan size of the image is 1 μm and the rms roughness of the film is 5.8 nm

the surface, and we have two limit cases of cluster deposition on the surface depending on the cluster energy. If this energy is sufficiently high, clusters are embedded into the upper surface layer and remain motionless until other deposited clusters form chemical bonds with them. In the other limit case, deposited clusters propagate along the surface up to the formation of chemical bonds with other clusters. In both cases, we assume the chemical bonds to be stronger between clusters than between clusters and the surface. We note that the criterion for each limit case is determined not only by the specific energy of incident clusters but also by the intensity of a cluster beam.

We first consider the limit case of embedded clusters that corresponds to a high energy of deposited clusters. In this case, the cluster is stuck with a solid, and its subsequent motion along the surface is hampered, as in experiments [26–28] with deposition of fast silver clusters on silicon and carbon surfaces. This corresponds to the deposition model where a deposited cluster is motionless, and we consider this model below. Because a deposited cluster does not change its position on the substrate surface and the point of its sticking has a random character, we have the following equation for the coverage of a substrate surface:

$$\frac{dS}{dn} = s\left(1 - \frac{S}{S_0}\right). \tag{4.1}$$

Here, S_0 is the total substrate area, S is the occupied area, s is the cross section of an individual monomer, and n is the number of monomers on the surface. To describe matter in this model, we throw some disks of area s on the surface. As a result of solving this equation, we obtain the degree of coverage

$$\xi \equiv \frac{S}{S_0} = 1 - \exp\left(-\frac{ns}{S_0}\right). \tag{4.2}$$

Comparing this model with observed data, we see that this model does not work in the framework of the fulfilled experiment, i.e., cluster monomers change their position in the course of aggregate formation. We therefore relate this model to the conditions of experiments in [26–28], and below we analyze the other limit case of cluster deposition. This model may be used

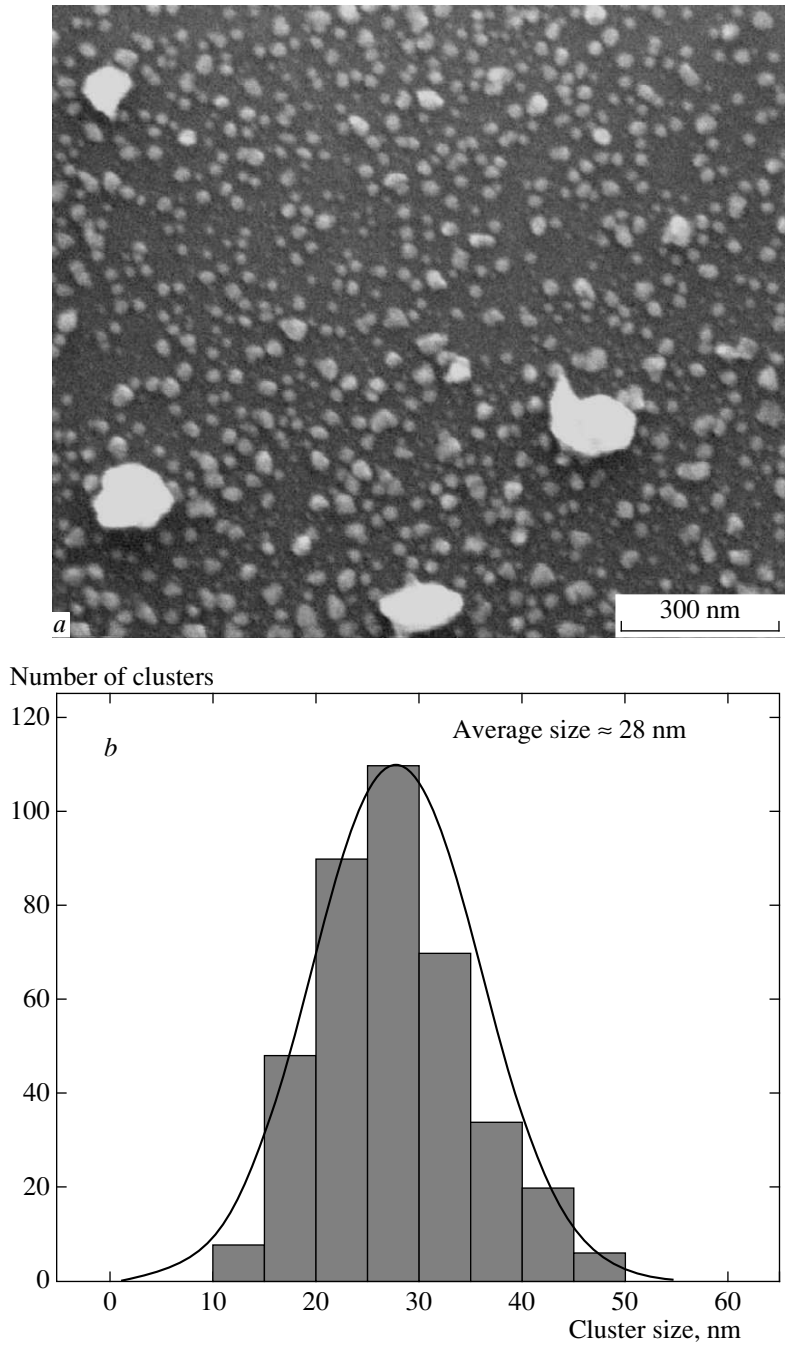

Fig. 4. Deposition of solid silver clusters with the diameter 4.1 nm for the exposition time 8 min. (a) SEM photography of a film; (b) the distribution function of surface aggregates with respect to diameters

in the case where solid clusters are strongly embedded into a solid, and subsequently deposited clusters contacting with them form bonds with these clusters. The aggregates formed under these conditions have the fractal dimension close to 3 [29, 30], i.e., this leads to formation of compact films. Of course, such films have pores, but these pores are minimal in accordance with the case of conservation of a shape of each solid cluster.

If the surface coverage by deposited clusters is low, their diffusion along the surface leads to the formation of fractal aggregates in accordance with the DLA model (diffusion-limited aggregation) [5–7] or DDA

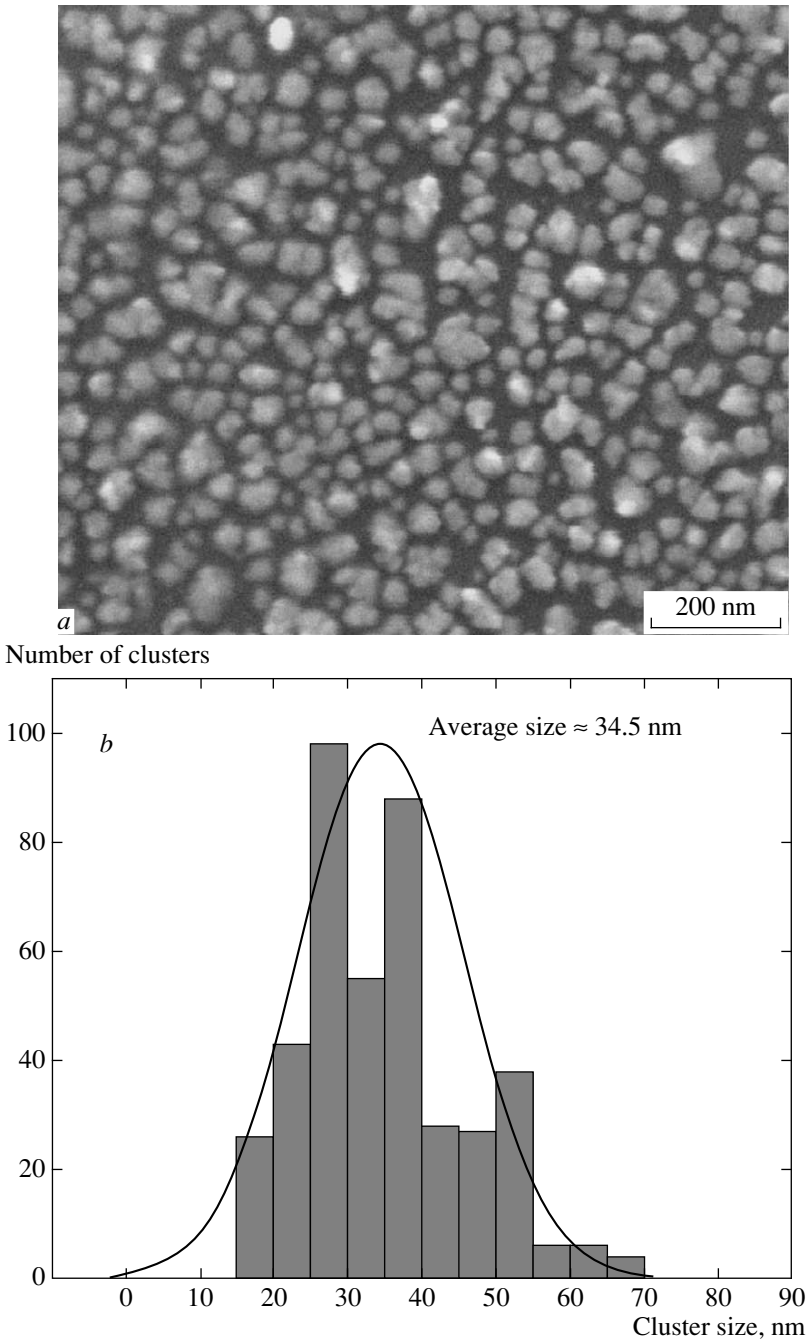

Fig. 5. Deposition of solid silver clusters of 5.6 nm in diameter for the exposition time 8 min. (a) SEM photography of a film; (b) the distribution function of surface aggregates with respect to diameters

model (deposition diffusion aggregation) [3] for these processes. The above models account for the diffusion motion of clusters over the surface and their joining in fractal aggregates with formation of strong chemical bonds at the points of their contact. These models, depending on certain conditions, are analyzed in books and reviews [8, 31, 32]. We are guided by the DLA model as regards the formation of a three-dimensional fractal aggregate. This model describes experimental structures resulting from cluster joining (see, e.g., [4, 33–35]). In our case, the applicability of this model means that after establishment a chemical

bond between two solid clusters, restructuring of a system of bound clusters proceeds. As a result, a test cluster is displaced and forms a chemical bond with other solid clusters of this aggregate. Therefore, each solid cluster in a fractal aggregate mostly preserves its structure, but has several nearest neighbors in a formed fractal aggregate.

The DLA model is rough in relation to the experimental conditions where the intensity of a cluster beam is relatively high and the formed film is not rarefied. But this description of cluster growth is supported by the fact that the measurements for silver aggregates on the silicon surface with AFM show that its shape is close to spherical. Below, we therefore model these structures as fractal aggregates with the fractal dimension $D = 2.46$. Considering the metal film to be composed of fractal aggregates formed according to the DLA model, we analyze some properties of this film from this standpoint. We let a denote the cluster radius and r the radius of the fractal aggregate; we then have the number of cluster monomers in a fractal aggregate [8, 31, 32]

$$\kappa = \left(\frac{r}{a}\right)^D, \tag{4.3}$$

where D is the fractal dimension of this cluster. Correspondingly, the area per cluster monomer is equal to

$$S_{cl} = \frac{\pi r^2}{\kappa} = \frac{\pi a^2 \kappa^{2/D}}{\kappa} = \frac{s}{\kappa^{1-2/D}}. \tag{4.4}$$

Under the experimental conditions, $r = 15$ nm and $a = 2.8$ nm, we have $\kappa = 62$. This implies that formation of clusters leads to a decrease in the absorbed (occupied) area by 2.2 times, which roughly corresponds to the data of the graph presented in Fig. 6.

We can analyze the size distribution of clusters on the surface in accordance with Fig. 6, which gives the size distribution for liquid clusters. The relation between the radius r of a fractal cluster and the radius R of a liquid cluster is given by

$$R = r^{D/3} a^{1-D/3} \tag{4.5}$$

in accordance with the definition of fractal dimension (4.3). Thus, the size distribution of liquid clusters gives the size distribution of initial clusters under the assumption that solid clusters are melted independently. But comparison of the distribution in Figs. 5 and 6 shows that in reality, several clusters are joined into one drop. Figure 6 allows finding the total specific mass of silver on a substrate. Because it is the same in the cases in Fig. 5 and Fig. 6 (i.e., this mass does not change on melting), we find that the porosities of clusters in Fig. 1*b* and 1*c* are equal. We can find the porosity by another method on the basis of the fractal structure of clusters,

$$\eta = \left(\frac{r}{a}\right)^{3-D}, \tag{4.6}$$

whence $R = 18$ nm ($a = 2.8$ nm, $D = 2.46$). It is necessary to explain that η in Eq. (4.6) is the ratio of the volume of a fractal aggregate to the volume occupied by solid clusters, i.e., $1/\eta$ is the volume part occupied by solid clusters. Thus, the size distribution of melted clusters allows reconstructing the size distribution of solid clusters. On average (with $a = 2.8$ nm, $r = 15$ nm, and $D = 2.46$), this formula gives η that corresponds more or less to the above operation. Thus, the average value is $\eta = 0.40$, i.e., pores occupy roughly 60 % of the aggregate volume, which corresponds to the data in Fig. 6.

5. DIFFUSION MODEL OF CLUSTER AGGREGATION

We consider the diffusion model of growth of cluster aggregates on a surface. In this model, we assume that solid clusters of a radius r are directed onto a surface and are merged there in aggregates. We let J denote the cluster beam flux to the surface, and let R be the current aggregate radius. For simplicity, we assume the aggregates to have a spherical shape and identical radii. Next, the coverage ζ of the surface by aggregates is assumed to be small,

$$\zeta = N\pi R^2, \tag{5.1}$$

where N is the current number density of aggregates on the surface. Each contact with an aggregate leads to attachment of a solid cluster to the aggregate, and subsequently this aggregate takes an almost spherical shape as a result of restructuring. Condition (5.1) means that the mean free path λ of clusters over a surface is relatively large,

$$\lambda = \frac{1}{2\pi RN} = \frac{R}{2\zeta} \gg R. \tag{5.2}$$

We characterize the diffusion motion of clusters over the surface by the length a of cluster motion on which the motion direction is changed and the time τ of displacement over this distance. Then the diffusion coefficient of clusters over the surface is

$$d \sim \frac{a^2}{\tau}. \tag{5.3}$$

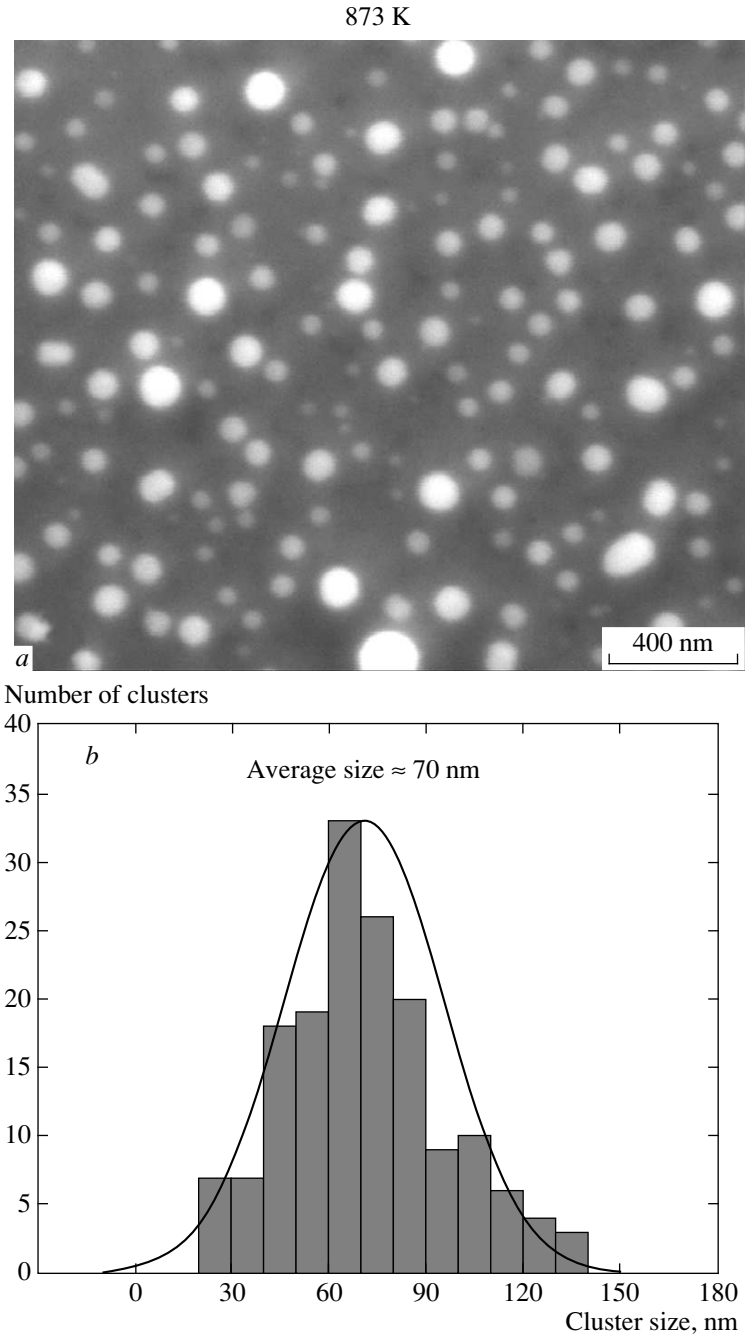

Fig. 6. (a) SEM image of solid silver nanoclusters with the diameter 5.6 nm for 6 min deposition after annealing at 873 K in nitrogen atmosphere for 3 min, and (b) the corresponding histogram to show the distribution function of surface aggregates with respect to diameters

We note that the diffusion character of cluster motion means that a typical distance L over which a cluster propagates before its attachment to an aggregate is

$$L \sim \sqrt{dt} \sim \sqrt{a\lambda} \ll \lambda, \tag{5.4}$$

where t is the lifetime of a cluster on the surface with respect to its attachment to aggregates. This gives the criterion for the diffusion character of cluster motion before its attachment:

$$\zeta \ll \frac{a}{R}. \tag{5.5}$$

We now analyze the experimental conditions from

the standpoint of the diffusion model of cluster aggregation. In the course of aggregate growth, a surface is initially free, and then the clusters deposited as a result of diffusion along the surface merge and form aggregates consisting of many clusters. We are guided by typical values of experimental data with the typical cluster radius $r = 5$ nm, the aggregate radius $R = 30$ nm, and the flux of incident clusters $J \sim 10^{10}$ cm$^{-2} \cdot$ s^{-1}. We derive the condition that an incident cluster attaches to an aggregate rather than to a cluster on the surface. Under this condition, the mean free path of a deposited cluster λ with respect to attachment to an aggregate much exceeds the path for attachment to a surface cluster λ_{cl}. In terms of the above parameters, the attachment time t_a of a surface cluster to an aggregate is $t_a \sim \lambda\tau/a$, and the number density of free solid clusters on the surface N_{cl} is given by

$$N_{cl} \sim Jt_a \sim \frac{J\lambda\tau}{a} \sim \frac{J\tau}{a}\,\frac{R\zeta}{a}.$$

From this, the condition that the mean free path for a free surface cluster to attach to another surface cluster $\lambda_{cl} = 1/(2\pi r N_{cl})$ be small compared to the mean free path λ for cluster attachment to aggregate is

$$\frac{RrJ\tau}{a\zeta} \ll 1. \tag{5.6}$$

If we use the parameters of this experiment and take $a \sim 1$ nm as a minimum value of this parameter, we obtain $\tau \ll 10^{-12}$ s at $\zeta \sim 1$, which corresponds to a typical time of molecular motion. This means that the diffusion regime of cluster motion along the surface in the course of aggregation occurs only in the case of a nonactivation character of cluster motion over the surface. This occurs only for a relatively weak interaction between a deposited cluster and the surface, if a cluster is not embedded deeply inside a solid. Evidently, this is fulfilled at the deposition energy 0.7 eV/atom of this experiment and is not fulfilled at higher cluster energies for the same sort of clusters and the surface [26–28].

Thus, under these experimental conditions, we can specify the character of aggregate growth that is similar to the formation of fractal structures on a surface when solid particles attach to a surface and can move over it. Then solid clusters are merged on a surface due to a contact between them, and when several clusters are joined in an aggregate, and its restructuring proceeds that leads to formation of three-dimensional aggregates in which each cluster has bonds with several nearest neighbors. Of course, the fractal cluster structure relates to a low density of aggregates on the surface. This is not fulfilled under these experimental conditions. Nevertheless, the formed porous structure more or less conserves fractal properties of aggregates that constitute a formed porous film. Therefore, the above diffusion model may be used for understanding the structure of a formed film and for estimating its parameters.

6. MELTING OF SURFACE CLUSTERS

Upon heating to the temperature 873 K (Fig. 1*d*), the film is separated in round drops because of melting. We note that this temperature is lower than the melting point of bulk silver ($T_m = 1235$ K); it is a common fact that the melting point of clusters is lower than that for a macroscopic system (see, e.g., [36]). We have that the melting point of clusters depends not only on the cluster size but also on the completeness of its structure, and a decrease of the cluster melting point is determined by surface phenomena. Because in this case the film structure is constructed from individual solid clusters, this conclusion regarding the melting point is valid for the silver film under consideration. We also note that melting of silver clusters was studied specially in [37–39], and the melting point of clusters in all the cases was lower than that for bulk silver.

The basic advantage of film melting in the course of its annealing consists in the conservation of the film in individual drops. It is simple to analyze this system after its solidification because in this case, SEM measurements allow determining the coverage of the surface and the size distribution function of drops. From this, we can find the total film mass, and because the film mass does not change upon melting, this allows finding the pore distribution for the initial porous film. In fulfilling this operation, we verify that the above concept of film construction of cluster aggregates is applicable. Moreover, the fractal structure of aggregates consisting of individual solid clusters in accordance with formula (4.3) corresponds roughly to the mass of liquid drops. Thus, the analysis of a melted film that is divided in round drops justifies our basic concept that the film formed consists of cluster aggregates. These aggregates include tens of individual solid clusters, and the fractal structure of these aggregates may be valid in essence.

Thus, transformation of a film as a result of its heating allows analyzing the character of film melting. The film consists of individual clusters that interact with the substrate surface weakly if the bond between clusters occupies a small part of the cluster surface. Therefore, this method gives the possibility of melting individual

clusters. In addition, we can study the character of the solid–liquid phase transition in this way. Indeed, due to mixing of different crystal structures, premelting may be observed below melting [40] (cluster softening below the melting point). Evidently, this effect is observed in this experiment, but it requires a more detailed investigation.

7. THE EVAPORATION STAGE

Heating of a deposited film leads to its partial evaporation, and the analysis of this process allows determining the parameters of cluster evaporation at high temperature. In this analysis, we assume the surface film to consist of individual clusters, i.e., the surface of cluster contacts to be small compared to the total area of the cluster surface. In addition, the total area of contacts between clusters and the surface is also relatively small. We can then consider the cluster behavior at high temperature in the framework of the liquid drop model [23], and the binding energy of atoms in clusters may be determined from experimental results.

Indeed, in the framework of the liquid drop model for the cluster, taking a liquid cluster to consist of $n \gg 1$ atoms (and hence its surface energy small), we define the total binding energy E_b in terms of both the volume and the surface cluster energy as [23]

$$E_b = \varepsilon_0 n - An^{2/3}. \tag{7.1}$$

In the case of silver, the specific binding energy of bulk silver is $\varepsilon_0 = 2.87$ eV, and the specific surface energy is $A = 2$ eV [23]. The rate constant of atom attachment to the cluster is

$$k_n = k_0 n^{2/3}, \quad k_0 = \pi r_W^2 \sqrt{\frac{T}{2\pi M}}, \tag{7.2}$$

where the temperature T is expressed in energy units, M is the atom mass, and $r_W = 0.166$ nm is the Wigner–Seitz radius for liquid silver. For silver at $T = 600$ K, we have $k_0 = 7.4 \cdot 10^{-12}$ cm^3/s. The rate of cluster evaporation $\nu_{ev}(T)$ is

$$\nu_{ev}(T) = k_0 n^{2/3} N_{sat}(T) \exp(\Delta\varepsilon / T n^{1/3}), \tag{7.3}$$

where $N_{sat}(T)$ is the number density of atoms for saturated vapor, with $N_{sat}(T) \sim \exp(-\varepsilon_0/T)$, and $\Delta\varepsilon = 2A/3$ accounts for a decrease in the atom binding energy due to surface energy.

We apply the above formulas to experimental conditions of evaporation of silver and silver clusters. In particular, at temperatures $T = 600$ K, 700 K, and 800 K, the saturated number density of atoms N_{sat} is respectively equal to 15 cm^{-3}, $1.3 \cdot 10^4$ cm^{-3}, and $1.2 \cdot 10^7$ cm^{-3}. From this, we have the balance equation for a decrease in the cluster size due to cluster evaporation

$$\frac{dn}{dt} = -\nu_{ev}(T). \tag{7.4}$$

Its solution gives the total time τ_0 of cluster evaporation

$$\tau_0 = \frac{9Tn^{2/3}}{2Ak_0 N_{sat}(T)} \exp\left(-\frac{2A}{3Tn^{1/3}}\right). \tag{7.5}$$

In particular, for the cluster radius $r = 1$ nm, at the temperatures $T = 600$ K, 700 K, and 800 K, we have the evaporation times $\tau_0 = 2 \cdot 10^5$, 1000, and 0.8 hours. An increase in the cluster radius twice leads to an increase in τ_0 by an order of magnitude. We also evaluate the cluster evaporation time at $T = 873$ K and $T = 1073$ K for the cluster radius $R = 25$ nm according to the data in Fig. 1 ($n \approx 3 \cdot 10^6$). In this case, the exponential in formula (7.5) is unity, $N_{sat}(873\text{ K}) = 6 \cdot 10^7$ cm^{-3}, $N_{sat}(1073\text{ K}) = 7 \cdot 10^{10}$ cm^{-3}, and $k_0 \approx 1 \cdot 10^{-11}$ cm^3/s. Then formula (7.5) gives the total evaporation time to be about 2 hours at $T = 1073$ K and three orders of magnitude higher at $T = 873$ K. This means that under the experimental conditions, several percent of silver is to be evaporated at $T = 1073$ K, and the evaporation process is not significant at $T = 873$ K.

The results concerning the evaporation of liquid drops on the surface can be used in another way. The rate of evaporation of a drop is sensitive to the binding energy of atoms located on the surface of the drop. The accuracy of values used is restricted, and therefore we now solve an inverse problem, with the experimentally observed parameters. In reality, we are based on two energetic parameters of surface atoms in accordance with formula (7.1), the bulk binding energy ε_0 and the specific surface energy A, and comparison of the drop distribution functions before and after evaporation allows determining both parameters in principle. Because we now deal with the average drop size only, we estimate a rough change of the binding energy ε_0 only. Based on the data in Fig. 6, we have that the drop size under annealing at $T = 1073$ K during 3 minutes decreases by approximately 20 %, which corresponds to the total evaporation time of about 13 min instead of 50 min as follows from formula (7.5) with the cluster parameters presented in [23]. We can obtain this value if we replace the binding energy $\varepsilon_0 = 2.87$ eV with the value $\varepsilon_0 = (2.74 \pm 0.03)$ eV, i.e., have this value

decreased by 5 %, which is probably within the limits of accuracy of the used data. The indicated accuracy takes into account that a part of the cluster surface does not partake in the evaporation process. Thus, this method can be used to determine the binding energy and the surface tension of small drops with high accuracy.

Thus, this method of evaporation of a porous film resulting from deposition of solid clusters onto a surface allows finding the parameters of evaporation for free clusters as well as the binding parameters of atoms in clusters.

8. CONCLUSION

The above analysis based on experimental studies allows describing the character of evolution of large solid clusters deposited on a surface if the energy of deposition is relatively small and the interaction energy between deposited clusters and the surface is small compared to the interaction energy of two contacted solid clusters. In this regime, clusters deposited onto a surface propagate along it as a result of diffusion, and merging of clusters onto the surface leads to formation of cluster aggregates. As a result of restructuring that increases the number of nearest neighbors for each bound cluster, these aggregates have a three-dimensional structure rather than a planar one. In addition, according to their structure, the formed cluster aggregates are close to fractal aggregates that are formed in a rarefied matter. Subsequent joining of neighboring aggregates by deposited solid clusters that attach to aggregates directly leads to formation of a porous film that is of interest for various applications. The parameters of this porous structure may be determined by annealing of the film, which leads to its melting and transformation into a set of separate compact particles on the surface. This program is partially realized above for deposition of solid silver clusters onto a silicon surface.

As follows from the above analysis and comparison with similar studies [26–28, 41], there is a variety of deposition regimes of solid clusters onto a surface that also depend on the deposition energy [15]. Energetic clusters are embedded deeply into a solid and are stuck there, whereas clusters of a relatively small energy are located on the surface and can move along it as a result of diffusion. The regime of cluster deposition affects the properties of a thin porous film formed. Therefore, the structure of a porous film resulting from deposition of given solid clusters onto a certain target may be adjusted by the energy of the deposited clusters. Subsequently, this affects the electric, optical, mechanical, and chemical properties of a formed porous film.

Understanding the character of film growth is of importance for nanotechnology because such films may be used as a medicine [14], catalysts [42], and nanoelectronic devices [43–45]. But the development of this kind of nanotechnology requires the development of methods for generation of cluster beams and diagnostic methods for nanostructures. In particular, this study includes a modern technique as a source of intense beams of selected metal clusters and scanning electron microscopy (SEM). All this, as well as X-ray methods for the analysis of surface chemistry, complicates such investigations. In addition, the method developed allows studying processes that involve cluster melting and evaporation. Indeed, the binding energy of atoms in an individual cluster is large compared to the interaction energy between this and neighboring clusters, and also between this cluster and a substrate. Therefore, processes of cluster melting and evaporation in a formed film are close to those involving free clusters. As a result, we have a method for determining cluster parameters, and this method is more reliable than those with cluster beams.

The authors thank Mr. S. Banerjee for technical assistances in operating the SEM and Mr. P. Mishra for AFM analysis. This work was supported in part by DFG, Germany and the RFBR, Russia (Grant 06-02-16146a). One of the authors (SRB) is grateful to Institut für Physik, Ernst-Moritz-Arndt Universität Greifswald, Germany for local hospitality to carry out the experiment in the Nanocluster Deposition facility.

REFERENCES

1. S. A. Kukushkin and V. V. Slezov, *Disperse Systems on Solid Surfaces*, Nauka, Petersburg (1996).

2. S. A. Kukushkin and A. V. Osipov, Phys. Uspekhi **168**, 1083 (1998).

3. P. Jensen, A. L. Barabási, H. Larralde, S. Havlin, and H. E. Stanley, Phys. Rev. **50B**, 15316 (1994).

4. A. Perez, P. Melinon, V. Dupuis, P. Jensen, B. Prevel, J. Tuaillon, L. Bardotti, C. Martet, M. Treilleux, M. Broyer, M. Pellarin, J. L. Vaille, B. Palpant, and J. Lerme, J. Phys. **30D**, 709 (1997).

5. T. A. Witten and I. M. Sander, Phys. Rev. Lett. **47**, 1400 (1981).

6. P. Meakin, Phys. Rev. **27A**, 604, 1495 (1983).

7. M. Sahimi, M. McKarnin, T. Nordahl, and M. Tirrell, Phys. Rev. **32A**, 590 (1985).

8. B. M. Smirnov, Phys. Rep. **188**, 1 (1990).

9. H. Gleiter, Nanostruct. Mater. **1**, 1 (1992).

10. H. Gleiter, Nanostruct. Mater. **6**, 3 (1995)

11. S. Y. Liau, D. C. Read, W. J. Pugh, J. R. Furr, and A. D. Russell, Lett. Appl. Microbiol. **25**, 279 (1997).

12. A. Gupta and S. Silver, Nature Biotechnol. **16**, 888 (1998).

13. K. Nomiya, A. Yoshizawa, K. Tsukagoshi, N. C. Kasuga, S. Hirakawa, and J. Watanabe, J. Inorg. Biochem. **98**, 46 (2004).

14. J. R. Morones, J. L. Elechiguerra, A. Camacho, K. Holt, J. B. Kouri, J. P. Ramirez, and M. J. Yacaman, Nanotechnology **16**, 2346 (2005).

15. C. Binns, Surf. Sci. Rep. **44**, 1 (2001).

16. K. Shintani, Y. Taniguchi, and S. Kameoka, J. Appl. Phys. **95**, 8207 (2004).

17. T. H. Lee, C. R. Hladik, and R. M. Dickson, Appl. Phys. Lett. **84**, 118 (2004).

18. I. Shyjumon, M. Gopinadhan, O. Ivanova, M. Quaas, H. Wulff, C. A. Helm, and R. Hippler, Eur. Phys. J. **37D**, 409 (2006).

19. B. M. Smirnov, I. Shyjumon, and R. Hippler, Phys. Rev. **77E**, 066402 (2007).

20. I. Shyjumon, M. Gopinadhan, C. A. Helm, B. M. Smirnov, and R. Hippler, Thin Solid Films **500**, 41 (2006).

21. B. M. Smirnov, I. Shyjumon, and R. Hippler, Phys. Scripta **73**, 288 (2006).

22. www.oaresearch.co.uk/cluster.htm

23. B. M. Smirnov, *Clusters and Small Particles in Gases and Plasmas*, Springer, New York (1999).

24. K. Siegbahn, *Alpha-, Beta- and Gamma-Ray Spectroscopy*, North Holland, Amsterdam (1965).

25. J. I. Goldstein, D. E. Newbury, P. Echlin, D. C. Joy, C. E. Lyman, E. Lifshin, L. Sawyer, and J. R. Michael, in: *Scanning Electron Microscopy and X-ray Microanalysis*, Kluwer, New York (2003).

26. S. J. Carroll, S. Pratontep, M. Streun, R. E. Palmer, S. Hobday, and R. Smith, J. Chem. Phys. **113**, 7723 (2000).

27. M. Couillard, S. Pratontep, and R. E. Palmer, Appl. Phys. Lett. **82**, 2595 (2003).

28. R. E. Palmer, S. Pratontep, and H. G. Boyen, Nature Mater. **2**, 443 (2004).

29. P. Meakin, J. Colloid Interface Sci. **102**, 491 (1985).

30. Z. Racz and M. Pischke, Phys. Rev. **31A**, 985 (1985).

31. R. Jullien and R. Botet, *Aggregation and Fractal Aggregates*, World Scientific, Singapore (1987).

32. T. Viszek, *Fractal Growth Phenomena*, World Scientific, Singapore (1989).

33. W. T. Elam et al., Phys. Rev. Lett. **54**, 701 (1985).

34. Y. Sawada, A. Dougherty, and J. P. Golub, Phys. Rev. Lett. **56**, 1260 (1986).

35. D. Grier et al., Phys. Rev. Lett. **56**, 1264 (1986).

36. B. M. Smirnov and R. S. Berry, *Phase Transitions of Simple Systems*, Springer, Berlin (2007).

37. T. Castro, R. Reifenberger, E. E. Choi, and R. P. Andres, Phys. Rev. **42B**, 8548 (1990).

38. S. Zhao, S. Wang, and H. Ye, J. Phys. Soc. Jpn. **70**, 2953 (2001).

39. H. Arslan and M. H. Güven, New J. Phys. **7**, 60 (2005).

40. C. L. Cleveland, W. D. Luedtke, and U. Landman, Phys. Rev. Lett. **81**, 2036 (1998).

41. S. Pratontep, S.J. Carroll, C. Xirouchaki, M. Streun, and R. E. Palmer, Rev. Sci. Instr. **76**, 045103 (2005).

42. A. T. Bell, Science **299**, 1688 (2003).

43. A. P. Alivisatos, Science **271**, 933 (1996).

44. C. S. Lent and P. D. Tougaw, Proc. IEEE **85**, 541 (1997).

45. S. O. Obare, R. E. Hollowell, and C. J. Murphy, Langmuir **18**, 10407 (2002).